UCRL- 2240 c.2

UNCLASSIFIED

UNIVERSITY OF CALIFORNIA — BERKELEY

TWO-WEEK LOAN COPY

This is a Library Circulating Copy which may be borrowed for two weeks. For a personal retention copy, call Tech. Info. Division, Ext. 5545

RADIATION LABORATORY

UCRL-2240 c2

mfc-37593

DISCLAIMER

This document was prepared as an account of work sponsored by the United States Government. While this document is believed to contain correct information, neither the United States Government nor any agency thereof, nor the Regents of the University of California, nor any of their employees, makes any warranty, express or implied, or assumes any legal responsibility for the accuracy, completeness, or usefulness of any information, apparatus, product, or process disclosed, or represents that its use would not infringe privately owned rights. Reference herein to any specific commercial product, process, or service by its trade name, trademark, manufacturer, or otherwise, does not necessarily constitute or imply its endorsement, recommendation, or favoring by the United States Government or any agency thereof, or the Regents of the University of California. The views and opinions of authors expressed herein do not necessarily state or reflect those of the United States Government or any agency thereof or the Regents of the University of California.

UCRL-2240
Unclassified - Physics
Distribution

UNIVERSITY OF CALIFORNIA

Radiation Laboratory

Contract No. W-7405-eng-48

ANGULAR DISTRIBUTIONS AND TOTAL CROSS SECTIONS FOR THE INELASTIC SCATTERING OF 31-MEV PROTONS FROM HEAVY ELEMENTS

Robert Martin Eisberg

(Thesis)

June 15, 1953

Berkeley, California

TABLE OF CONTENTS

		Page
Abstract		3
I.	Introduction	4
II.	Experimental Details	10
III.	Experimental Results	25
IV.	Conclusions	45
V.	Acknowledgments	49
VI.	Bibliography	50

ANGULAR DISTRIBUTIONS AND TOTAL CROSS SECTIONS FOR THE INELASTIC SCATTERING OF 31-MEV PROTONS FROM HEAVY ELEMENTS

Robert Martin Eisberg

Radiation Laboratory, Department of Physics,
University of California, Berkeley, California

June 15, 1953

ABSTRACT

Angular distributions and total cross sections for the inelastic scattering of 31 Mev protons from four heavy elements, Pb, Au, Ta, and Sn, have been measured. Differential cross sections were obtained at five angles: 30°, 45°, 60°, 90°, and 135°.

The differential cross sections are strongly peaked forward, increasing by about a factor of ten as the scattering angle goes from 135° to 30°.

The total cross sections all have values ranging from 0.25 barns, for Sn, to 0.29 barns, for Pb.

ANGULAR DISTRIBUTIONS AND TOTAL CROSS SECTIONS FOR THE INELASTIC SCATTERING OF 31-MEV PROTONS FROM HEAVY ELEMENTS

Robert Martin Eisberg

Radiation Laboratory, Department of Physics,
University of California, Berkeley, California

June 15, 1953

I. INTRODUCTION

Inelastic scattering of high energy protons is a technique which has been used since about 1940 to investigate the energy structure of nuclei. The procedure involves bombarding thin targets of the element to be investigated with mono-energetic protons and, at some angle with respect to the incident beam, observing the energy distribution of the scattered protons.

When targets of low atomic number are used, the energy spectra of the scattered protons are usually found to consist of several discrete energy groups.[1] The most energetic group contains the elastically scattered particles and is found at an energy a little below that of the incident particles. This is due to the energy imparted to the recoil of the target nucleus. The less energetic proton groups, which are referred to as the inelastic groups, correspond to collisions in which the target nucleus has absorbed some of the kinetic energy of the incident proton and is thus left in a state of excitation. The scattering of the inelastic protons into a discrete spectrum of energies is a direct consequence of the fact that, as a quantum mechanical system, the nucleus can exist only in a discrete spectrum of states of excitation. In the center of mass system the energy of the incident proton, less the energy of the inelastically scattered proton, must equal the energy absorbed by the target nucleus. Thus, from the observed laboratory system energy

spectrum, one may easily infer information about the spectrum of energy levels of the target nucleus. This process should be contrasted with a somewhat similar one that occurs in an experiment such as the resonant absorption of slow neutrons. In the latter case, the energy of the incident particle is varied and information is obtained on the energy level structure of the compound nucleus. In the case of inelastic scattering, the energy of the emitted particle is the variable and information is obtained on the energy level structure of the target nucleus.

As the excitation of a nucleus is increased, the average spacing between energy levels will, in general, decrease due to the increasing complexity of the modes of excitation and the consequent increase in the number of possible modes. Thus, at sufficiently high bombarding energies, it is found that the spectrum of the lower energy inelastically scattered protons is continuous, representing the excitation of the target nucleus to its continuum.

Since the war, a great deal of experimental work has appeared in the literature in which most of the light elements through aluminum have been investigated with bombarding energies usually in the region of four to eight Mev (a few experiments have been reported from the Princeton cyclotron at 17 Mev and from the Berkeley linear accelerator at 31 Mev).[2, 3, 4, 5]

To investigate inelastic proton scattering from elements of medium and high atomic weight it is necessary to use bombarding energies somewhat higher than eight Mev as may be seen from the following considerations. The region of the energy level spectrum of the target nucleus which may be investigated by inelastic proton scattering extends from zero energy up to an energy equal to the kinetic energy of the incident proton diminished by an energy roughly equal to the height of the Coulomb barrier of the target nucleus. This is because the emission of inelastically scattered protons from the region of the target nucleus, of energies less than that of the Coulomb barrier, will be greatly impeded due to the small probability of Coulomb barrier penetration. The height of the Coulomb barrier of lead for protons is about 14 Mev and it

decreases with Z, the atomic number, being given approximately by the formula

$$V_{coulomb} = Z/A^{1/3} \qquad \text{(in Mev)}$$

where A is the atomic weight. Thus inelastic proton scattering experiments on the heavier elements could hardly be performed by the investigators working at eight Mev.

As the atomic number of a nucleus takes on successively larger values, the average spacing of the energy levels of the nucleus decreases. The fine structure of the energy spectra of alpha particles from the natural alpha emitters indicates that the average spacing of the first few levels of the nuclei at the top end of the periodic table is of the order of a hundred kilovolts. Thus, using apparatus of moderate resolving power, one would expect that the observed energy spectrum of protons inelastically scattered from a heavy element would entirely consist of a continuous spectrum, as contrasted to the case of inelastic scattering from light elements. The information that one would expect to obtain about the heavy elements from inelastic scattering, consequently, differs from that obtained about light elements. For the light elements, inelastic proton scattering provides the location of discrete energy levels -- for the heavy elements, it could be expected to provide information about the density of levels.

The anticipated connection between the energy spectrum of inelastically scattered protons and the energy level density of the target nucleus is obtained by considering the model of the compound nucleus.[6, 7] According to this model, the incident proton enters the target nucleus (Z, A) and rapidly shares its kinetic energy with the nucleons of the target nucleus forming the compound nucleus (Z + 1, A + 1) which is excited to an energy equal to the kinetic energy of the incident proton plus its binding energy to the compound nucleus. This, in general, excites the compound nucleus into the continuum. The compound nucleus will de-excite itself in a time of the order of 10^{-15} seconds by emitting one or possibly several nucleons. These nucleons are evaporated in a Maxwellian-like distribution corresponding to a temperature of the compound nucleus determined by its excitation energy and its atomic weight. The

angular distribution of the emitted nucleons will be isotropic in the case in which the residual nucleus is left excited in the continuum. (In any case arguments based upon conservation of angular momentum and parity indicate that the angular distribution will be symmetrical about 90° in the center of mass.[8])

For the emission of protons by the compound nucleus of high Z the Coulomb barrier has a very pronounced effect. In the case of lead excited by 31 Mev protons, the temperature of the compound nucleus is about 1.3 Mev while the Coulomb barrier is about 14 Mev high. Neutrons will be emitted from the compound nucleus with a Maxwellian-like distribution maximizing at about 2.6 Mev, but protons will have an energy distribution in which the probability of emission of a proton, of kinetic energy E, is very small for E small compared to the Coulomb barrier height and which, as E increases, rises in the typical exponential barrier penetration form. The probability will maximize when E is a little less than the height of the Coulomb barrier and will then fall approximately according to the exponential $e^{-E/kT}$, where kT = 1.3 Mev.

The exact shape of the energy spectrum for the case of single nucleon emission is given by a simple argument involving detailed balancing between an initial state consisting of the compound nucleus, and the final state consisting of the residual nucleus plus emitted nucleon. (It can be modified to handle multiple nucleon emission.)

$$P(E)\,dE = C\,E\,\frac{dN(\epsilon)}{d\epsilon}\,\sigma_c(E)\,dE$$

where,

$P(E)\,dE$ = number of nucleons emitted per unit time in energy interval dE at energy E

$\frac{dN(\epsilon)}{d\epsilon}$ = density of energy levels of residual nucleus at its excitation energy ϵ

$\sigma_c(E)$ = capture cross section of residual nucleus for nucleons of energy E forming the compound nucleus

$\sigma_c(E)$ may be written as

$$\sigma_c(E) = \pi R^2 f(E)$$

where,

πR^2 = geometrical cross section of residual nucleus

$f(E)$ = Coulomb barrier penetration probability

The behaviour of $\frac{dN(\epsilon)}{d\epsilon}$ has been predicted by several models. These give $\frac{dN(\epsilon)}{d\epsilon} = Ke^{A\sqrt{\epsilon}}$; K and A are constants. This would give rise to the Maxwellian-like distribution mentioned above.

The purpose of an inelastic scattering experiment on a heavy element would be, presumably, to measure the shape of the inelastic energy distribution carefully, and from this to deduce the function $\frac{dN(\epsilon)}{d\epsilon}$ which describes the energy dependence of the level density of the residual nucleus. This could then be compared with the results predicted by the several models. Experimental information on $\frac{dN(\epsilon)}{d\epsilon}$ would be of great theoretical interest for, at present, the only information that exists for heavy elements is the level density in the region of low excitation, as inferred from alpha emission fine structure, and the level density in the region of eight Mev, as measured in neutron capture resonance experiments.

Some of the first experiments on inelastic proton scattering from heavy elements were done several years ago by Roy Britten at the Berkeley linear accelerator.[9] Using a sodium iodide scintillation spectrometer, he observed the energy spectrum of 31.5 Mev protons scattered inelastically at 90° from Pt and Pb. His results were surprising, for they indicated that the energy spectrum of the inelastic protons was not of the Maxwellian character predicted by the compound nucleus theory. Instead, the spectrum was quite flat. In addition to this, the differential cross section which he obtained at 90° was at least an order of magnitude larger than that predicted by the compound nucleus theory. At about the same time, similar experiments (unpublished) were carried out, also on the Berkeley linear accelerator, by Benveniste, Levinthal,

Martinelli, and Silverman. In these experiments, Pt and Bi were bombarded and the inelastic proton spectra were obtained by range measurements. The results of these experiments also showed that the energy distribution was not Maxwellian-like. Furthermore, these workers found indications of inelastic protons scattered off at energies lower than the very appreciable Coulomb barriers of Pt and Bi would seem to allow. It was not possible to use the work of Britten, whose spectra did indicate the expected Coulomb barrier cut-off, to disprove these data because Britten's measurements on the lower energy protons were unreliable. This was due to the fact that the background rate of pulses in the single sodium iodide crystal used by Britten, of the size of the pulses given by the lower energy protons, was very much larger than the counting rate of scattered low energy protons. Britten obtained his spectra by a target in - target out subtraction technique which, for the low energy part of the spectra, was not very satisfactory as it involved looking for a small difference in two large numbers.

In the fall of 1951, an experiment was started by the present author, in conjunction with George J. Igo, to check the results of Britten and of Benveniste, et al. In this experiment, 31 Mev protons were scattered from Pb and the inelastically scattered protons were analyzed at 90° to the incident beam by a two counter telescope consisting of a proportional counter followed by a sodium iodide scintillation counter. Only scintillation counter pulses were analyzed which came in time coincidence with a pulse from the proportional counter corresponding to the passage of a heavily ionizing particle through the counter and on into the scintillation counter. This technique effectively eliminated the large background of low energy pulses which troubled Britten. The results of this experiment showed that Britten's work was essentially correct.[10] The shape of the energy spectrum was quite flat down to the Coulomb barrier cut-off, which occurred at about the expected energy. The value of the differential cross section for the process was in good agreement with Britten's and, therefore, was very much larger than that predicted by the compound nucleus theory.

The experiment described herein is essentially an amplification of the experiment using a two counter telescope, mentioned above. The

method of determining the ionization of the particle, whose energy is to be measured by the scintillation counter, has been improved by using three proportional counters, so that a sampling of the ionization much closer to the mean ionization is obtained. This permits the identification of the mass of the particle detected, instead of simply discrimination against direction and uncharged radiation or electrons, which was all that was really possible in the original experiment. In this experiment, 30.6 Mev protons were scattered from four elements: Sn, Ta, Au, and Pb. Energy distributions of scattered particles were obtained, for each element, at each of six different angles: 15°, 30°, 45°, 60°, 90°, and 135°. At each energy interval (in most cases) a five point pulse height analysis was run on the ionization pulses to look for a heavily ionizing component which would represent deuterons.

II. EXPERIMENTAL DETAILS

1. The Linear Accelerator

The Berkeley linear accelerator is ideally suited as a proton source for heavy element scattering experiments. It produces a mono-energetic beam of approximately 31 Mev protons confined to a very narrow bundle of small angular divergence. The beam is emitted in pulses of about 300 microseconds duration at a repetition rate of 15 cps. Thus, it has a duty cycle (time "on" per second) of approximately 1/2 percent, which is quite adequate for experiments using proportional counters, sodium iodide scintillation counters, and electronic circuitry involving one microsecond pulses. In the highly collimated geometry used, the available time average beam current is of the order of 10^{-8} amperes, which is somewhat more than could be used in this experiment.

2. Bombardment Geometry

Fig. 1 shows the geometry of collimators, target, counter, and Faraday cup as used in the experiment. The stripping foil consists of a 1/4 mil aluminum foil which is inserted in the beam ahead of the analyzing magnet. Its purpose is to break up singly ionized hydrogen molecules, which can be produced at about 16 Mev by the linear acceler-

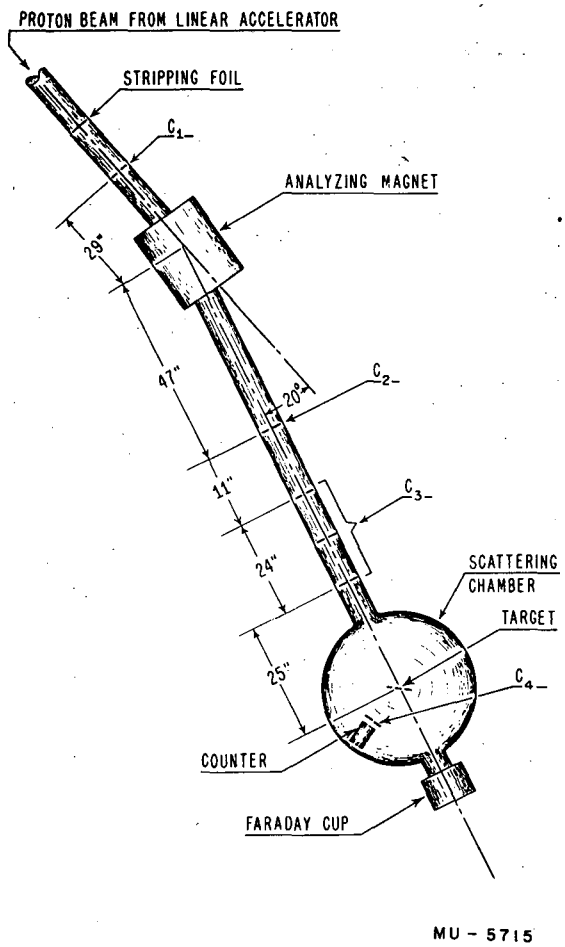
PROTON BEAM FROM LINEAR ACCELERATOR
STRIPPING FOIL
C_1
ANALYZING MAGNET
29"
47"
20°
C_2
11"
C_3
24"
SCATTERING CHAMBER
TARGET
25"
C_4
COUNTER
FARADAY CUP
MU - 5715

Fig. 1

ator, into two 8 Mev protons which are then removed from the beam by the analyzing magnet. The collimator C_1 is used to control the beam current. It is generally set at about 1/8 in. by 1/8 in. After passing through the analyzing magnet the beam is collimated roughly by C_2, which is set at about 3/16 in. by 3/16 in. Collimator C_3 consists of three carbon disks spaced one foot apart. The first disk has a 1/8 in. hole, the second and third have 3/16 in. holes. The collimator is constructed so that the three holes are very accurately coaxial. The first disk gives the beam its final shape. The second and third disks do not scrape the main beam, but act as baffles to remove protons which are scattered from the edges of the first disk. Carbon is used in C_3 because its low Z gives a favorable ratio of stopping power to multiple Coulomb scattering, and because its high (p, n) threshold makes it a poor source of background neutrons.

The targets consist of thin foils, 3/4 in. high and 1-1/4 in. wide, placed at the center of the scattering chamber at 45° to the incident beam. The counter telescope may be set at any desired angle with respect to the incident beam. Particles scattered from the target are required to pass through one more collimator, C_4, before entering the detecting counters. This collimator, which determines the solid angle involved in the calculation of cross sections from the data, is mounted at the front of the counter telescope. It consists of a 3/32 in. hole in a steel plate located at 5-11/16 in. from the center of the target. This defines the solid angle to be 2.13×10^{-4} steradians.

To monitor the beam passing through the target, a Faraday cup is mounted on the exit port of the scattering chamber. The Faraday cup, scattering chamber, and the pipe containing the collimators are all evacuated. The pumping is done by the linear accelerator vacuum system and by an auxiliary pump connected to the scattering chamber.

Before each run, the entire apparatus is carefully aligned with the aid of a transit. The apparatus is sufficiently well braced that it cannot easily come out of alignment.

3. <u>The Scattering Chamber</u>

In the early stages of the experiment it was decided to construct a

somewhat elaborate scattering chamber which would allow the experimenter to change targets, and to change the azimuthal positions of the target and the counter, by remote control in a manner which would always maintain the vacuum of the scattering chamber. Despite the high cost of such a piece of apparatus, it was apparent that it would pay for itself in a very short time by greatly increasing the fraction of scheduled bombardment time actually used in obtaining data. The specifications for the scattering chamber were drawn up by George J. Igo and the author, aided by the advice of Drs. Alvarez, Benveniste, and Martinelli. The engineering design was done by Mr. Roy Marker. The chamber was built in a very short time and was put into operation in the fall of 1952.

Fig. 2 shows a schematic diagram of the scattering chamber. The evacuated volume consists of a circular cylinder two feet in diameter and one foot high. The incident beam passes through the chamber eight inches above the base. The counters are mounted on a circular table which is capable of rotating through 360° and is driven by a motor. Along the vertical axis of the cylinder is a shaft which supports a frame which can hold eight targets. Motors drive the shaft up and down and cause it to rotate. The azimuthal and vertical location of the target holder and the azimuthal position of the table are indicated at the remote control panel by a system of selsyns and microswitches. The scattering chamber may be evacuated to a pressure of the order of 10^{-5} mm. of Hg by means of a self contained pump unit. Fig. 3 shows the scattering chamber, pump, collimator C_3, and the Faraday cup. Fig. 4 shows the remote control panel.

4. Beam Integration

The beam passing through the target was collected in a Faraday cup mounted on the exit port of the scattering chamber. Since it was desired to use targets as thick as possible in order to increase the ratio of inelastic protons to background, it was necessary to consider the possibility of multiple Coulomb scattering in the target throwing some of the beam out of the Faraday cup. To within 10 or 15 percent, the root mean square angle of multiple Coulomb scattering of protons by thin foils is

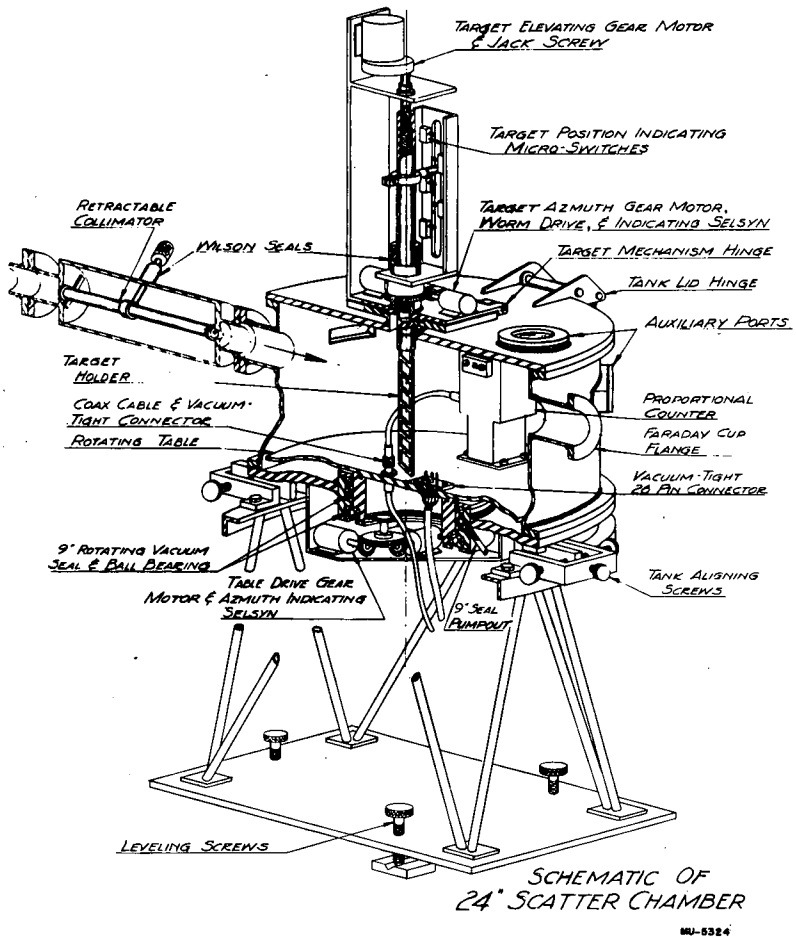
TARGET ELEVATING GEAR MOTOR & JACK SCREW
TARGET POSITION INDICATING MICRO-SWITCHES
RETRACTABLE COLLIMATOR
WILSON SEALS
TARGET AZMUTH GEAR MOTOR, WORM DRIVE, & INDICATING SELSYN
TARGET MECHANISM HINGE
TANK LID HINGE
AUXILIARY PORTS
TARGET HOLDER
COAX CABLE & VACUUM-TIGHT CONNECTOR
ROTATING TABLE
PROPORTIONAL COUNTER
FARADAY CUP FLANGE
VACUUM-TIGHT 20 PIN CONNECTOR
9" ROTATING VACUUM SEAL & BALL BEARING
TABLE DRIVE GEAR MOTOR & AZMUTH INDICATING SELSYN
9" SEAL PUMPOUT
TANK ALIGNING SCREWS
LEVELING SCREWS
SCHEMATIC OF 24" SCATTER CHAMBER
MU-5324

Fig. 2

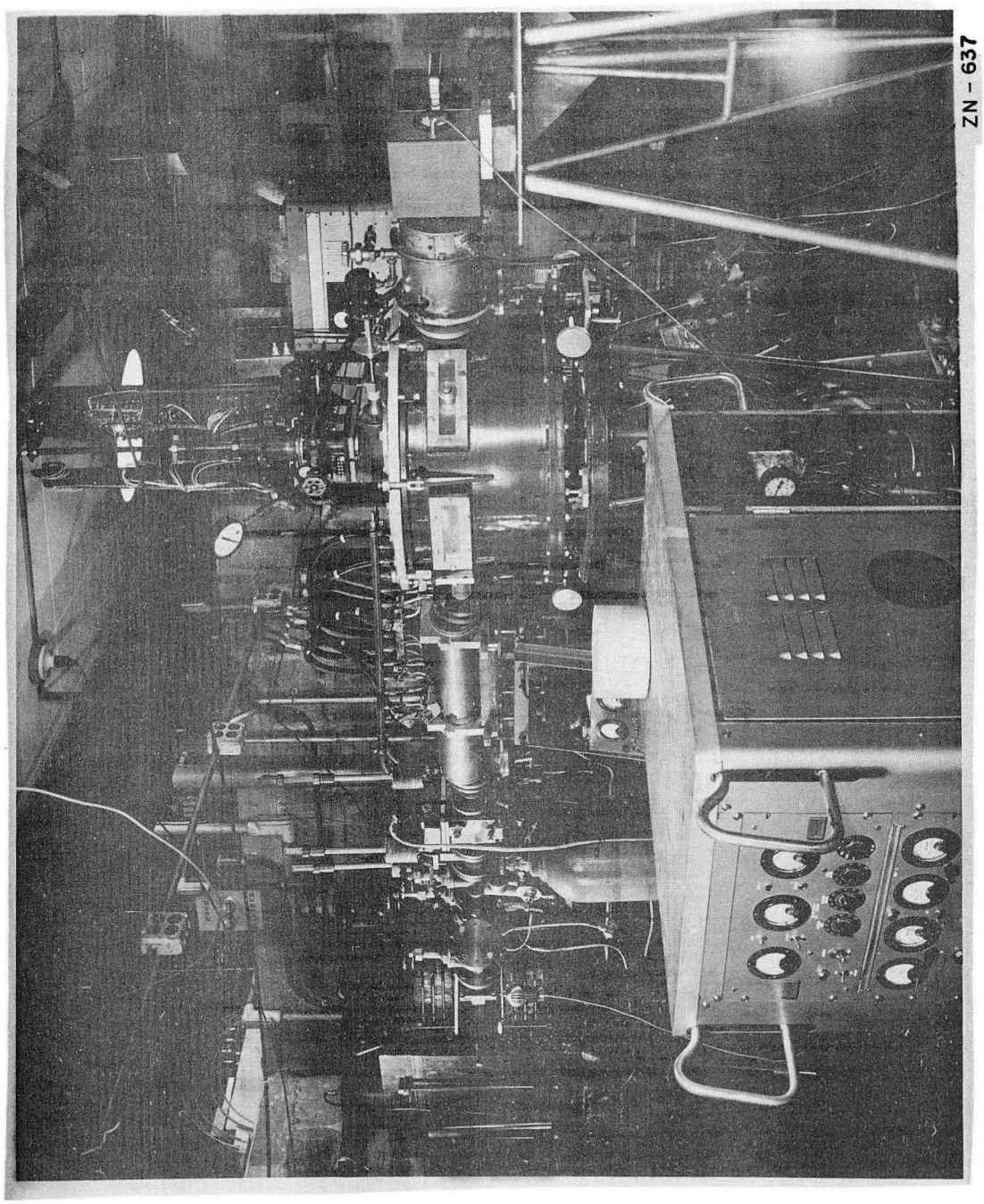

Fig. 3

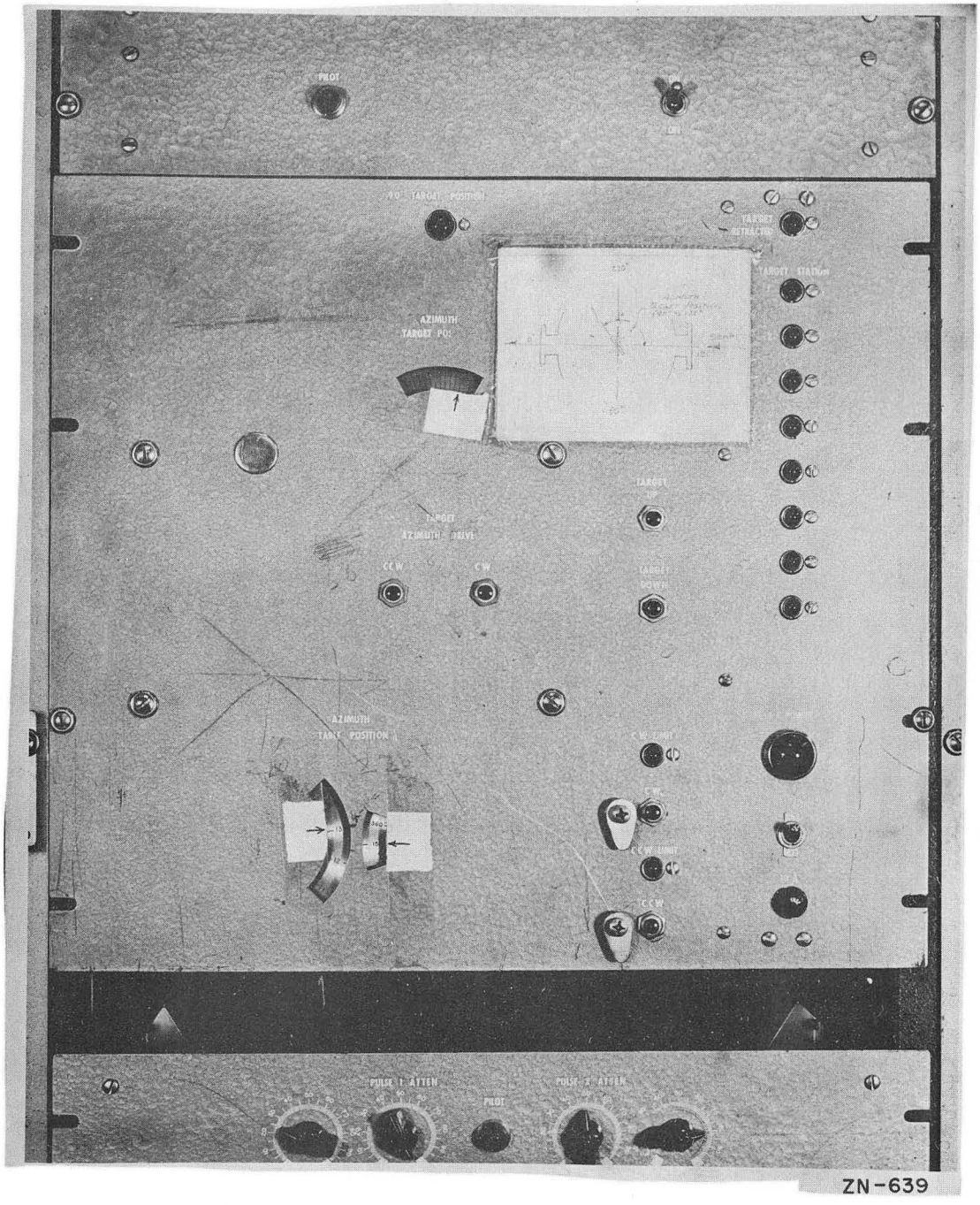
PILOT
TARGET POSITION
TARGET RETRACTED
TARGET STATION
AZIMUTH TARGET POS
TARGET UP
TARGET AZIMUTH DRIVE
CCW
CW
TARGET DOWN
AZIMUTH TARGET POSITION
CCW
PULSE 1 ATTEN
PILOT
PULSE 2 ATTEN
ZN-639

Fig. 4

given by:

$$\left(\overline{\theta^2}\right)^{1/2} = \left(\frac{dE}{E} \quad \frac{Z}{1800}\right)^{1/2}$$

where,

$\left(\overline{\theta^2}\right)^{1/2}$	=	rms scattering angle
dE	=	energy loss in traversing foil
E	=	kinetic energy of proton
Z	=	atomic number of foil

Using this expression, it was calculated that the rms scattering angle, for the three heavy targets Ta, Au, and Pb, was $2.0 \pm 0.1 \times 10^{-2}$ radians. For Sn the rms scattering angle was 1.6×10^{-2} radians. A Faraday cup was obtained which had an aperture defined by a 2-3/4 in. hole located 22 in. from the target position. This allows the cup to intercept all of the beam, multiply Coulomb scattered from the heavy targets at an angle less than three rms scattering angles.

To prevent secondary electrons from escaping the Faraday cup, two large Alnico horseshoe magnets were placed to provide a transverse field of several hundred gauss over the surface of the cup struck by the beam. A second pair of magnets placed in front of the Faraday cup served to prevent any electrons, that might be in the beam, from entering the cup.

The charge collected on the Faraday cup was measured by a feedback integrating electrometer. The feedback voltage, V, is applied to a recording voltmeter. The operation of the feedback circuit is such that the effect of the capacitance of the Faraday cup and the cable is negligible compared to the capacitance, C, of the condenser in the electrometer circuit. Consequently the charge, Q, collected is given by the expression $Q = CV$. C was measured to be 0.0101 microfarads.

5. Targets

Four targets were used in the experiment: Sn ($Z = 50$), Ta ($Z = 73$), Au ($Z = 79$), and Pb ($Z = 82$). It is not possible to obtain a thin foil of an element located about half way between $Z = 50$ and $Z = 73$ because this is the region of the rare earths. The only thin (1/2 mil) uranium foil that

could be procured had the appearance of a thin slice of swiss cheese. This made it impossible to obtain an accurate measurement of the areal density of the region of the target bombarded. Consequently uranium was not used.

To maximize the ratio of scattered protons to background, the foils were made as thick as possible subject to two restrictions. First, multiple Coulomb scattering of the incident beam by the target could not be so great that the available Faraday cup would not be large enough to intercept the beam. Second, the targets could not be so thick that the uncertainty introduced in determining the energy of the lowest energy protons expected, due to the uncertainty in their point of origin in the target, was the determining factor in the energy resolution of the experiment. It happened that either of these criteria, taken alone, gave about the same result for the optimum target thickness. The optimum areal density came out to be 40 milligrams/cm^2. Two of the foils were obtained from stock, the other two were obtainable only in relatively thick foils and required rolling to bring their areal density below the specified limit.

Rectangular pieces of foil were cut. The area and mass of the pieces were measured. These pieces were then used as targets. The measured areal densities are given below.

Element	Areal Density
Sn	37.5 mgm/cm^2
Ta	27.9 "
Au	36.9 "
Pb	39.2 "

(These figures include a factor of $\sqrt{2}$ arising from the fact that the targets were placed at an angle of 45° to the incident beam.)

6. The Scintillation Counter

Protons scattered from the targets first pass through the proportional counters and then enter the thallium activated sodium iodide crystal. When charged particles enter such crystals, they have the property of producing a flash of light of an intensity proportional to the energy lost by the particle in the crystal.[11] The light emitted by the crystal is di-

rected to the photo-cathode of an RCA 5819 photomultiplier tube. This tube will then produce a pulse of current which charges up a condenser to a voltage which is proportional to the energy expended by the charged particle in the crystal. Thus, by making the crystal thick enough to stop protons of all energies up to 31 Mev, one has a counter which can not only detect protons but can measure their energy.

The greatest difficulty in using sodium iodide as a scintillator arises from the fact that it is deliquescent. After several months of experimentation, the following technique was developed. A stubby quartz light pipe in the shape of a truncated cone is cemented, in optical contact, to the face of the 5819 tube. In a dry box, the sodium iodide crystal is cleaved to the shape of a cube approximately 5/8 in. on an edge. The crystal is then cemented, in optical contact, to the flat face of the light pipe with a cement known as Bonding Agent R-313 (made by Carl H. Biggs Co., Los Angeles, California). This cement is ideal for the purpose. It dries in several hours after the addition of a hardener. When dry it is very clear and hard. It does not attack sodium iodide. Next a cap of 1/4 mil aluminum foil is placed over the crystal and the slant sides of the light pipe. This serves to direct all the light to the photomultiplier. Then a vacuum tight housing is slipped over the assembly and sealed to the end of the 5819 tube by means of a gum rubber gasket. The device is then removed from the dry box and the housing is evacuated. Protons can pass through a thin window in the housing and enter the crystal. Using this technique, the crystal will be preserved indefinitely.

7. The Proportional Counters

Before entering the scintillation counter, the scattered protons traverse a set of three identical proportional counters. Each counter consists of a grounded cylindrical shell, 3/4 in. internal diameter and 3 in. long, with a 0.003 in. stainless steel wire located along the axis of the cylinder. The wire is supported at each end by disks of teflon and is maintained at a positive potential of 1900 volts. The cylindrical volume is filled with a mixture of 96 percent A and 4 percent CO_2. The narrow bundle of scattered protons passes through the counter perpendicular to its axis and straddling the wire.

As a charged particle traverses such a counter, it will lose kinetic energy by exciting and ionizing atoms of the gas through which it passes. Some of the electrons knocked out of the gas atoms will have enough kinetic energy to ionize additional gas atoms. When these more energetic electrons have expended their energy, the total number of ion pairs in the gas will be proportional to the energy lost by the charged particle. For argon, there will be 39 ion pairs created for each kev of energy lost by the charged particle.

Under the influence of the electric field created by the positive potential on the central wire, the electrons will drift rapidly toward the wire and the positive ions will drift much more slowly to the grounded shell. For the counter described, the time required for the electrons to drift to the vicinity of the wire is of the order of one tenth of a microsecond. For a cylindrical geometry, the electric field strength varies as the reciprocal of the distance from the center of the wire. Within a region surrounding the central wire, of dimensions equal to several wire diameters, the field strength is so large that the electrons drifting toward the wire can pick up enough energy, between collisions with the atoms of the gas, to ionize these atoms. Thus the total number of electrons collected by the central wire will be some multiple of the number of electrons which drift into the multiplying region. For the counter described, the multiplication constant is of the order of 100. The charge collected builds up a voltage across the capacitance of the counter and the cable connecting the counter to the amplifier. As the above discussion indicates, this voltage will be proportional to the energy lost by the charged particle in traversing the counter.

The mean rate of energy loss of a particle in traversing matter can be expressed as a function of its kinetic energy, charge, and mass. Thus, at kinetic energies of 31 Mev, a deuteron will have a mean rate of energy loss 1.7 times larger than that of a proton and about 25 times larger than that of an electron. As the kinetic energy is decreased, the ratio of the mean energy loss of deuterons compared to protons remains about 1.7, while the ratio for deuterons compared to electrons increases as the reciprocal of the kinetic energy. Consequently, by correlating the heights of pulses from the scintillation counter and one of the proportional

counters, it should be possible to determine the mass of the particle detected. In practice it is not possible to do this using only one proportional counter because of the very large statistical fluctuations in the energy loss of charged particles, of energies encountered in this experiment, in traversing a proportional counter of a reasonable thickness.[12] The frequency distribution of the energy loss of 31 Mev protons in traversing a 3/4 in. counter is a skew, bell-like curve with a full width, at half maximum, of about 50 percent and with a very pronounced tail extending to the high energy losses.[13] This distribution (in particular the presence of the tail) is too broad to allow adequate resolution of protons and deuterons. However, by using three proportional counters to sample the ionization of the particle three times, it is possible to achieve a much more accurate estimate of the mean ionization of the particle. This information is treated by sending the three proportional counter pulses into a circuit which selects the smallest pulse. The output of this circuit is then used to represent the mean ionization of the particle.

The three proportional counters are machined from a solid block of brass and are evacuated and filled from a common port. The entrance window is a 1/4 mil Al foil, 1/8 in. in diameter. There are no foils between the first and second and the second and third counters. The exit window of the third counter and the entrance window of the scintillation counter are sufficiently larger than 1/8 in. so that multiple Coulomb scattering, of the lowest energy particles detected, in the entrance window and counter gas will not deflect them out of the counter telescope.

Fig. 5 shows the counter telescope mounted inside the scattering chamber.

8. The Electronics

Fig. 6 shows a block diagram of the electronic set up used in the experiment. The detected protons traverse proportional counters 2, 3, and 4 in succession and then stop in the scintillation counter (XTAL). The pulses from the counters are first fed into shorted delay line clipping units (CLIP) which provide rectangular pulses, one microsecond long, whose heights are proportional to the size of the counter pulses.

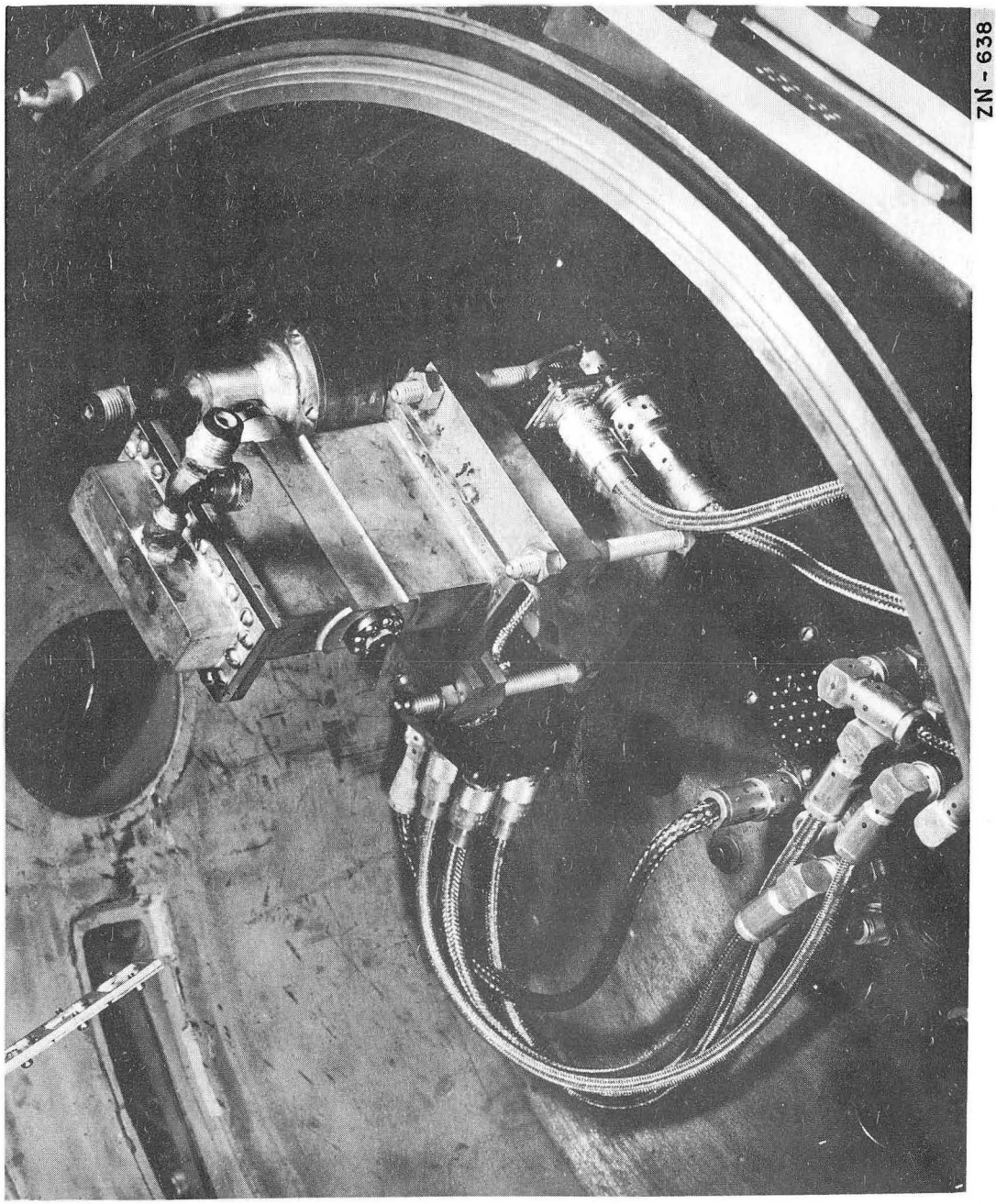

Fig. 5

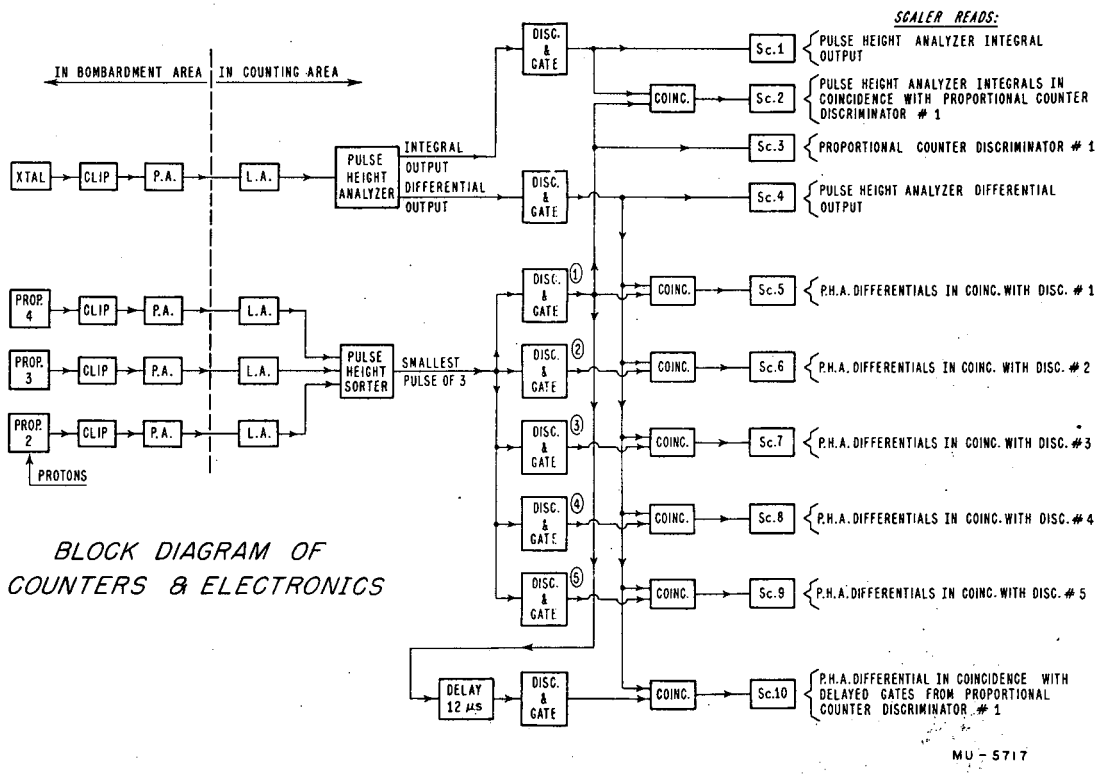
SCALER READS:
IN BOMBARDMENT AREA
IN COUNTING AREA
XTAL
CLIP
P.A.
L.A.
PULSE HEIGHT ANALYZER
INTEGRAL OUTPUT
DIFFERENTIAL OUTPUT
DISC. & GATE
COINC.
Sc.1
PULSE HEIGHT ANALYZER INTEGRAL OUTPUT
Sc.2
PULSE HEIGHT ANALYZER INTEGRALS IN COINCIDENCE WITH PROPORTIONAL COUNTER DISCRIMINATOR # 1
Sc.3
PROPORTIONAL COUNTER DISCRIMINATOR # 1
Sc.4
PULSE HEIGHT ANALYZER DIFFERENTIAL OUTPUT
PROP. 4
PROP. 3
PROP. 2
PROTONS
PULSE HEIGHT SORTER
SMALLEST PULSE OF 3
Sc.5
P.H.A. DIFFERENTIALS IN COINC. WITH DISC. # 1
Sc.6
P.H.A. DIFFERENTIALS IN COINC. WITH DISC. # 2
Sc.7
P.H.A. DIFFERENTIALS IN COINC. WITH DISC. # 3
Sc.8
P.H.A. DIFFERENTIALS IN COINC. WITH DISC. # 4
Sc.9
P.H.A. DIFFERENTIALS IN COINC. WITH DISC. # 5
DELAY 12 μs
Sc.10
P.H.A. DIFFERENTIAL IN COINCIDENCE WITH DELAYED GATES FROM PROPORTIONAL COUNTER DISCRIMINATOR # 1
BLOCK DIAGRAM OF COUNTERS & ELECTRONICS
MU-5717

Fig. 6

The pulses are then sent through pre-amplifiers (PA) and linear amplifiers (LA).

The scintillation counter pulses are fed into a one channel pulse height analyzer (PHA). This unit has two outputs: integral and differential. A pulse will appear in the integral output whenever the scintillation counter pulse is higher than a level determined by the lower discriminator. The differential output will deliver a pulse whenever the scintillation counter pulse is higher than the level determined by the lower discriminator and lower than the level determined by the higher discriminator. The level of the lower discriminator may be varied in such a way that the separation between the lower discriminator level and the higher discriminator level is held constant. The integral and differential outputs are fed into units containing a discriminator and a circuit giving an output gate of variable length (DISC. and GATE).

The three proportional counter pulses are fed into a pulse height sorter which provides an output pulse whose height is proportional to the height of the smallest of the three input pulses. The output of this circuit is fed to the inputs of five DISC. and GATE units. Unit number 1 is set so that it will produce a gate whenever a particle of ionization equal to, or greater than, that of a 31 Mev proton traverses the proportional counters. The discriminators of units 2 through 5 are set at successively higher levels and are used to run a five point pulse height analysis on the proportional counter pulses.

The outputs of DISC. and GATE 1 through 5 are put into coincidence with pulses from the PHA differential output in the coincidence circuits (COINC). The coincidence circuit outputs are fed to scalers (SC). The output of DISC. and GATE number 1 is also put into coincidence with the PHA integral output. In addition, the output of DISC. and GATE number 1 is used to trigger a delay circuit which in turn produces a gate of the same length as the gate from DISC. and GATE 1, but delayed by 12 microseconds. This delayed gate is put into coincidence with the PHA differential output gate and is used to determine the contribution of accidental coincidences to the counts recorded by the coincidence circuit fed by the PHA differential output and the output of DISC. and GATE 1. Finally the unmixed differential and integral PHA counts are recorded

as well as the counting rate of DISC. and GATE 1.

Although this set up seems a little complex, each part is necessary either to provide required data or to provide a continuous check on the operation of the equipment. The way in which the various scaler readings are used, and some of the reasons why they are necessary, will be explained in the next section.

III. EXPERIMENTAL RESULTS

1. Measurement of Beam Energy

Prior to the first experimental run, the linear accelerator beam energy was measured. An absorber wheel was placed in front of the Faraday cup, and the current collected in the cup was measured as a function of the thickness of aluminum absorber. The incident beam was monitored by counting protons elastically scattered from a thin foil placed in front of the absorber wheel. During this experiment, the current in the analyzing magnet was measured. Small changes in beam energy at a subsequent time can then be determined by noting the corresponding changes in magnet current required to steer the beam through the fixed geometry of collimators.

During the experimental runs, the beam energy was 30.6 ± 0.3 Mev.

2. Proportional Counter Plateaus

The first thing to be done in a run is to set DISC. and GATE 1 so that it will produce a gate whenever a heavily ionizing particle traverses the three proportional counters. To do this, the counter telescope is set at some forward angle, such as 30°, and an analysis is run on the energy of the detected particles with the pulse height analyzer. The pulse height analyzer is then set so that it will produce a pulse in its differential output channel only when an elastically scattered proton enters the counter telescope. At forward angles this is very easy to do since most of the detected particles are elastically scattered protons. Next the counting rate, of the output pulses of the coincidence circuit fed by DISC. and GATE 1 and the PHA differential output, is measured as a function of the bias on the discriminator of DISC. and GATE 1. When

the beam intensity is kept at a reasonable level, a very nice plateau will be obtained. An example is shown in Fig. 7. This curve, when differentiated, gives the frequency distribution of pulse heights from the circuit which selects the smallest of the three proportional counter pulses -- pulses being measured only when a 31 Mev proton traverses the proportional counters. The derivative is a gaussian-like curve with a full width at half maximum of about 30 percent. This is a much narrower distribution than is obtained when only one proportional counter is used.

Having obtained a discriminator bias plateau, the bias of DISC. and GATE 1 is set to be well up on the plateau, as indicated in Fig. 7. The unit will then produce a gate whenever a 31 Mev proton traverses the proportional counters. Since the specific ionization of a particle increases with decreasing energy and increasing mass, DISC. and GATE 1 will also produce a gate whenever a lower energy proton or deuteron traverses the proportional counters.

3. Search for Deuterons

By spotting DISC. and GATE units 1 through 5 at appropriate points on the discriminator bias plateau, it is possible to get a very good idea of the shape of the curve in one run. At each setting of the pulse height analyzer, the discriminator biases were so adjusted. Thus there was obtained, at each point of the energy spectrum, a plateau such as in Fig. 7. The presence of deuterons could be distinguished by the presence of a double step plateau, i.e.:

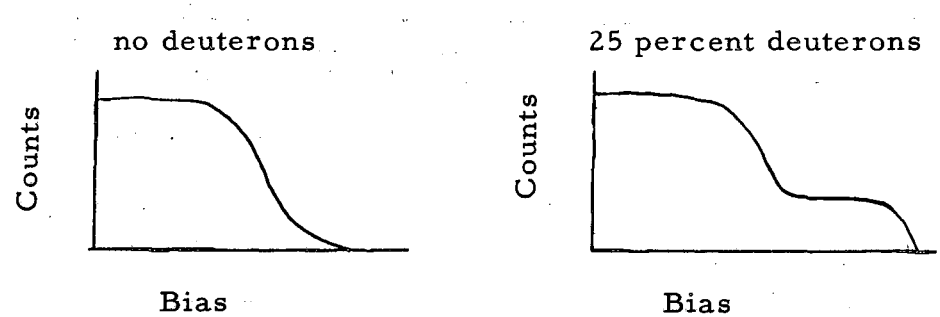

The results of these measurements indicate that, of the total number of inelastic heavy charged particles emitted when Sn, Ta, Au, or Pb are bombarded by 31 Mev protons, less than 10 percent are deuterons.

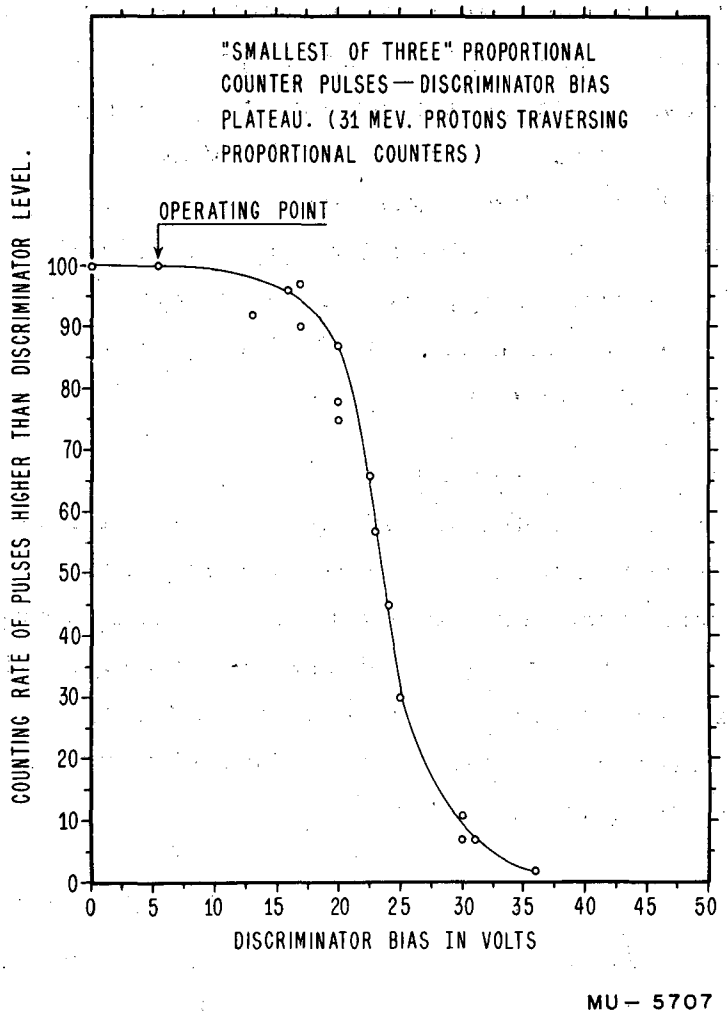
"SMALLEST OF THREE" PROPORTIONAL COUNTER PULSES — DISCRIMINATOR BIAS PLATEAU. (31 MEV. PROTONS TRAVERSING PROPORTIONAL COUNTERS)
OPERATING POINT
COUNTING RATE OF PULSES HIGHER THAN DISCRIMINATOR LEVEL.
100
90
80
70
60
50
40
30
20
10
0
0
5
10
15
20
25
30
35
40
45
50
DISCRIMINATOR BIAS IN VOLTS
MU-5707

Fig. 7

These data are described in detail in the thesis of George J. Igo.

4. Typical Energy Spectra

Fig. 8 shows a typical energy spectrum -- lead at 90°. The large peak at 31 Mev contains the elastically scattered protons. The hump, below the solid line, contains the inelastically scattered protons. Curve a, which fuses into the solid curve at about 18 Mev, represents the energy distribution of all pulses in the sodium iodide crystal. Curve b, which fuses into the solid curve at about 12 Mev, represents crystal pulses which are in time coincidence with a gate from DISC. and GATE 1. Thus one sees that below about 15 Mev most of the crystal counts are due to background. The higher energy background pulses are undoubtedly due to pile up of the more numerous lower energy pulses. Curve c represents the rate of accidental coincidences between crystal pulses, of a particular energy, and the gates from DISC. and GATE 1. The accidentals are measured with the delayed coincidence unit shown in Fig. 6. The solid curve is the difference between curve b and curve c. It represents the coincident crystal pulses, with accidental coincidences subtracted out -- thus the points on the solid curve give the counting rate of real inelastic protons.

As the scattering angle decreases towards zero, the cross section for elastic scattering increases very rapidly. Consequently, the complete energy spectrum will have a very different appearance at small angles. Fig. 9 shows the energy spectrum for gold at 30°.

5. Calculation of Cross Sections

Determining the differential cross sections from the energy spectra is simply a matter of counting the total number of inelastic protons and miltiplying by a factor determined by the number of nuclei per cm^2, the number of bombarding protons, and the solid angle accepted by the counter telescope. To determine the number of inelastic protons it is necessary to take into account the finite resolving power of the scintillation counter for the elastically scattered protons (approximately 8 percent full width at half maximum). The most reasonable method for doing this involves assuming that the resolution curve for the instrument is symmetrical about its maximum point.. The upper half of the elastic peak is reflect-

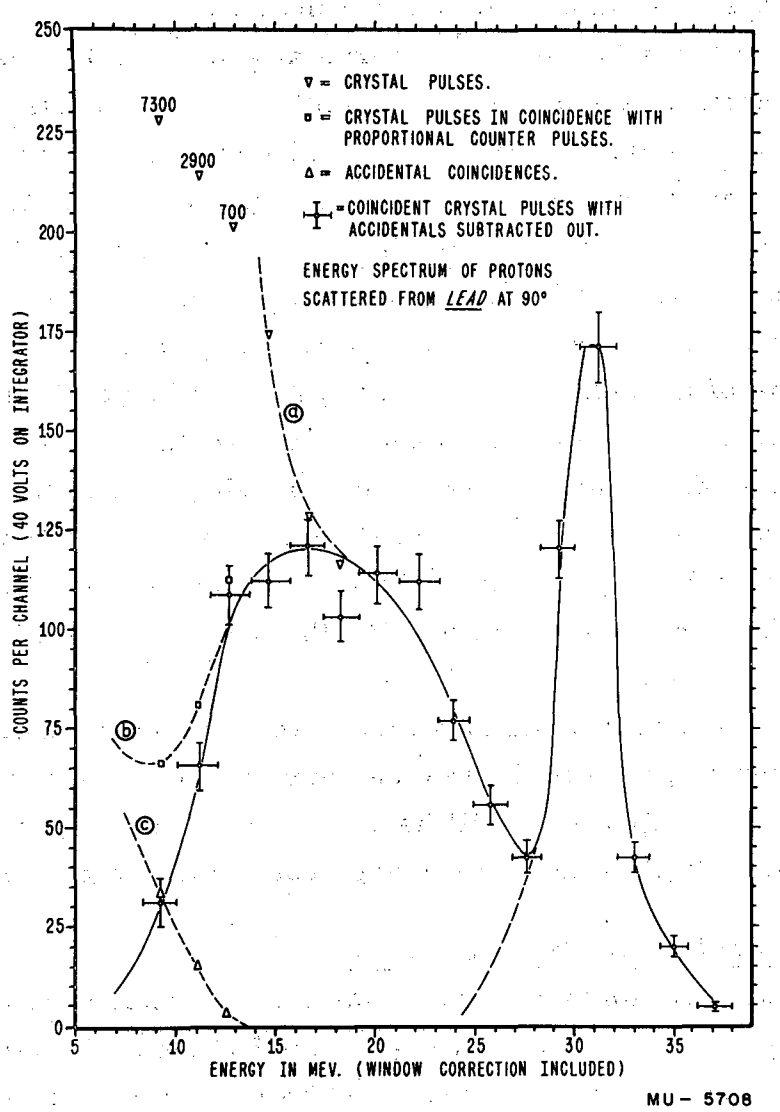
▽ = CRYSTAL PULSES.
▫ = CRYSTAL PULSES IN COINCIDENCE WITH PROPORTIONAL COUNTER PULSES.
Δ = ACCIDENTAL COINCIDENCES.
= COINCIDENT CRYSTAL PULSES WITH ACCIDENTALS SUBTRACTED OUT.
ENERGY SPECTRUM OF PROTONS SCATTERED FROM LEAD AT 90°
7300
2900
700
a
b
c
COUNTS PER CHANNEL (40 VOLTS ON INTEGRATOR)
ENERGY IN MEV. (WINDOW CORRECTION INCLUDED)
MU- 5708

Fig. 8

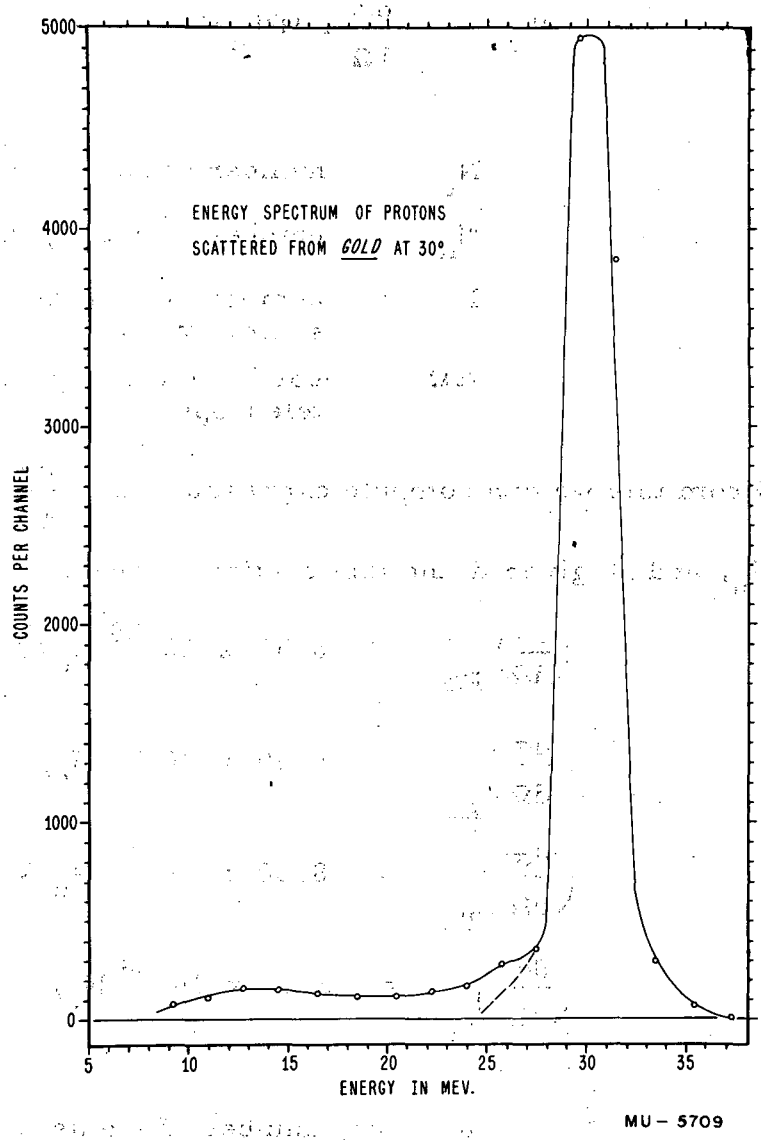
ENERGY SPECTRUM OF PROTONS
SCATTERED FROM GOLD AT 30°
COUNTS PER CHANNEL
5000
4000
3000
2000
1000
0
5
10
15
20
25
30
35
ENERGY IN MEV.
MU-5709

Fig. 9

ed about its maximum and the wing of the curve extending into the region of inelastic protons is subtracted out. The reflection process is indicated in Figs. 8 and 9.

The differential cross section is defined by the equation:

$$N_c = \frac{d\sigma}{d\Omega} \Delta\Omega N_n F$$

where,

N_c	=	number of scattered protons detected
N_n	=	number of nuclei/cm^2 in scatterer
F	=	number of protons incident upon scatterer
$\Delta\Omega$	=	solid angle accepted by counter telescope

From this we can compute expressions for $\frac{d\sigma}{d\Omega}$, using values for $\Delta\Omega$, N_n, and F given in the last section. The results are:

$$\left(\frac{d\sigma}{d\Omega}\right)_{Pb} = 6.53 \times 10^{-28} N_c/V$$

$$\left(\frac{d\sigma}{d\Omega}\right)_{Au} = 6.60 \times 10^{-28} N_c/V$$

$$\left(\frac{d\sigma}{d\Omega}\right)_{Ta} = 8.00 \times 10^{-28} N_c/V$$

$$\left(\frac{d\sigma}{d\Omega}\right)_{Sn} = 3.91 \times 10^{-28} N_c/V$$

where,

N_c	=	number of inelastic protons detected
V	=	voltage to which the Faraday cup electrometer circuit condenser is charged

The total cross section for a particular element may be calculated from the expression:

$$\sigma = \int \frac{d\sigma}{d\Omega} d\Omega .$$

Since, in this experiment, information about the differential cross sections is obtained at only six angles, the integral must be approximated by a sum. To do this, the unit sphere is divided into six zones centered about the polar angles at which the differential cross sections were measured. The solid angle of each zone is computed and then the total cross section is calculated from the expression:

$$\sigma = \sum_i \left(\frac{d\sigma}{d\Omega}\right)_i \Delta\Omega_i$$

Table I lists the zones and their solid angles.

Table I

Zone	Central polar angle	Range of polar angle	Solid angle
I	15°	$0^\circ - 22.5^\circ$	0.483
II	30°	$22.5^\circ - 37.5^\circ$	0.817
III	45°	$37.5^\circ - 52.5^\circ$	1.16
IV	60°	$52.5^\circ - 75^\circ$	2.19
V	90°	$75^\circ - 112.5^\circ$	4.03
VI	135°	$112.5^\circ - 180^\circ$	3.88

6. Discussion of Errors and Uncertainties

To arrive at the total uncertainty in the measured cross sections due to the various sources of error, one considers the formula for the differential cross section:

$$\frac{d\sigma}{d\Omega} = \frac{N_c}{\Delta\Omega N_n F}.$$

The solid angle is calculated from the equation: $\Delta\Omega = \frac{\pi r^2}{R^2}$

where r is the radius of the collimator hole, and R is the distance of the hole from the target. Both of these distances have a possible error of about 1 percent. Therefore $\Delta\Omega$ is uncertain to about 4 percent.

N_n, the number of target nuclei, is given by the expression:

$$N_n = \frac{N_{Avagadro}}{A} \sqrt{2}\ \rho$$

where ρ is the areal density of the target. The mean density of the foil is known to about 1/2 percent, but the density of the region of the foil bombarded by the beam is probably known to only about 2 percent.

F, the number of protons incident upon the scatterer, has uncertainty contributed from three sources: calibration and linearity of the integrating electrometer, calibration of the condenser in the circuit, human error in throwing the "count - stop" switch at the proper time. The magnitude of these errors are estimated to be, respectively, 1/2 percent, 1/2 percent, and 1 percent.

N_c, the number of inelastically scattered protons, also has possible error contributed from three sources. First, there is the statistical fluctuation in the number of inelastic protons counted. In all the spectra, the number of inelastic protons is of the order of 1000, so the statistical errors are about 3 percent. Second, there is error involved in resolving the elastic and inelastic protons. It is estimated that this error varies from about 3 percent for the 90° spectra to about 10 percent for the 30° spectra. Third, there is a source of error in the possible low energy contamination of the beam and in possible slit scattering in the counter telescope. These effects constitute the largest source of uncertainty for the small angle differential cross sections and must be discussed in detail.

Collimator C_3, with all its baffles, was designed to minimize the possibility of slit scattered protons of degraded energy from remaining in the beam and striking the scattering foil. However, the experiment is, by its very nature, extremely sensitive to beam contamination. This is because any low energy component of the beam can Coulomb scatter from the target nuclei. At the small angles, the Coulomb scattering

cross section becomes very large -- and, at low energies, the $1/E^2$ dependence of the Coulomb cross section makes it even larger. Thus, at the forward angles, any low energy beam contamination will have a high cross section for scattering into the counter telescope where it would be indistinguishable from inelastically scattered protons.

Similar spurious results would obtain if there was any appreciable amount of slit scattering in the collimator C_4 which defines the solid angle accepted by the counter telescope. This is because slit scattering of elastic peak protons would degrade their energy and cause them to be recorded by the scintillation counter as inelastic protons. The restricted space available inside the scattering chamber precludes the possibility of using a baffle type collimator for C_4 as was done for C_3.

To analyze the data one must find some way to take these two effects into account. Fortunately this may be done unambiguously by using the 15° energy distributions as a background run, so to speak. As an example, one would plot the 15° gold energy distribution on the same axes as the 30° gold energy distribution, but with the ordinates contracted so that the area under the elastic peak of the 15° spectrum equals the area under the elastic peak of the 30° spectrum. Then the two curves would be very similar except that the low energy part of the 15° spectrum contains approximately 50 percent of the area of the low energy part of the 30° spectrum, i.e., the spectra would have the appearance shown in Fig. 10.

Now, if one assumes that all of the low energy part of the 15° spectrum is due to slit scattering or beam contamination, then approximately 50 percent of the low energy part of the 30° spectrum is due to real inelastic protons, the rest being due to slit scattering or beam contamination. On the other hand, if one assumes that all of the low energy part of the 15° spectrum is due to real inelastic protons, then there can be no contribution from slit scattering or beam contamination to the 30° spectrum. Thus the true inelastic scattering cross section at 30° is bounded between 50 percent and 100 percent of the value indicated by the raw data.

Now the low energy part of the 15° spectrum is certainly not all due to real inelastic protons. Firstly, if it were then the inelastic cross section would increase by about a factor of 20 in going from 30° to 15°.

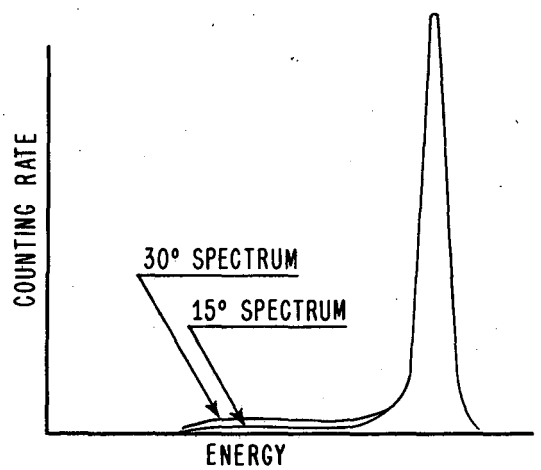

MU-5710

Fig. 10

This does not correlate with the behavior of the differential cross section at other angles. Secondly, since, in the 15° spectrum, the counting rate per energy interval in the low energy region is only about 1/2 percent of the counting rate per energy interval in the elastic peak, it is reasonable to expect that some of these low energy protons are due to slit scattering or beam contamination. On the other hand, the low energy part of the 15° spectrum is certainly not entirely due to slit scattering or beam contamination. This is true because at 30° these effects give roughly the same contribution to the spectrum as do real inelastic protons, and because the cross section for inelastic proton scattering will be seen to be increasing fairly rapidly with decreasing angle at these angles.

Consequently, a reasonable estimate to make is that the correct value for the inelastic scattering cross section for gold at 30° lies somewhere near the center of the allowed range of 50 percent to 100 percent of the uncorrected value. Consideration of the other elements at 30° gives very similar results, while at angles greater than 30° these effects are of rapidly decreasing importance.

At 30° the true value of the inelastic cross section is taken to be 75 percent of the value given by the raw data. The limits of error are ± 25 percent. At 45° the true value is taken to be 90 percent of the raw data value. The limits of error are ± 10 percent. Beyond 45° these effects are negligible.

As is indicated above, the energy spectra taken at 15° are of little value in determining the true inelastic cross sections. Consequently 15° cross sections will not be quoted in this paper. However, to determine the total cross section, an estimate of the 15° cross section must be obtained. This will be done by extrapolation from a smooth curve through the larger angle differential cross sections. This extrapolated value can be in error by as much as a factor of two.

To round up the discussion of uncertainties in the differential cross sections, it will be convenient to group the various sources of error into two types: (1) errors which would cancel out in a comparison of differential or total cross sections for the various elements, and (2) errors which would not cancel out in a comparison of the cross sections for the various elements. In the first group fall the sources of error due to:

$\Delta\Omega$, the electrometer, measurement of the condenser, and the error involved in the correction due to slit scattering and beam contamination. The second group consists of the errors due to: measurement of the density of the scatterer, operation of "count - stop" switch, statistical fluctuations, and the resolving power of the scintillation. Table II gives the quadratic sums of the errors of each type, and the quadratic sums of all errors.

Table II

Angle	Errors which cancel in comparison of cross sections for various elements	Errors which will not cancel	Total error
30°	25%	11%	27%
45°	11%	8%	14%
60°	4%	6%	7%
90°	4%	5%	6%
135°	4%	5%	6%

The large values of the total probable error for the measurement of the differential cross sections at small angles reflect the fact that it is difficult to obtain information about a relatively small number of inelastic protons in the presence of an overwhelming number of elastic protons.

The error in the total cross section for inelastic scattering is calculated by taking a straight arithmetical average of the suitably weighted errors of the differential cross sections. The weighting factor, for a particular angle, is proportional to the product of the differential cross section and the solid angle for that angle. Since the actual values of the errors in the total cross sections depend on the shape of the differential cross section curve, these errors will not be quoted until the total cross sections are presented.

Since the total error involved in the measurement of a particular differential cross section is compounded from a number of sources of error which are independent, it is reasonable to compute the total error

by taking a quadratic sum of the various contributing errors. However, it would not be correct to do the same in computing the error involved in the measurement of a total cross section, since the total errors in the differential cross sections are not independent.

The data was collected in two separate runs, the second about a month later than the first. In the first run a vital part of collimator C_4 was inadvertently left out. This caused an undue amount of slit scattering in C_4 which manifested itself in the 15° and 30° spectra, and to a small extent in the larger angle spectra. Taking into account the condition of collimator C_4 in the first run, the data of the two runs are in excellent agreement -- with one exception, Au at 45°. In the second run this differential cross section appeared to be about half the size obtained in the first run. This discrepancy is far outside the possible error and it is felt that some mistake was made in using the equipment at that point in the second run. Consequently no cross section is presented for Au at 45°. To calculate the total cross section for Au, the differential cross section at 45° will be obtained by interpolation. The data presented herein are taken from the second run.

As an additional check on the reproducibility of the results, the energy spectrum obtained from Pb at 90° in this experiment can be compared with that obtained in the experiment mentioned in the introduction. In the latter case a completely different group of apparatus was used -- no single item was used in both experiments except for the linear accelerator. The results of the two experiments are in excellent agreement, both as to the shape of the energy distribution and as to the differential cross section.

7. Differential Cross Sections

Table III lists the differential cross sections obtained in the experiment for the inelastic scattering of 31 Mev protons. For obvious reasons the results have been rounded off as follows: 0 - 10 mbn, rounded off to nearest 1/10 mbn; 10 - 20 mbn, rounded off to nearest 1/2 mbn; greater than 20 mbn, rounded off to nearest mbn. The fourth column contains the data uncorrected for slit scattering and beam contamination. The

Table III

Element	Angle	N_c/V	$\frac{d\sigma}{d\Omega}$ (millibarns/ster.)	$\frac{d\sigma}{d\Omega}$ (corrected for slit scattering etc.)
Pb	135°	644/100	4.2	4.2
	90°	919/40	15.0	15.0
	60°	1144/30	25	25
	45°	1496/20	49	44
	30°	1377/10	90	67
Au	135°	965/100	6.4	6.4
	90°	815/40	13.5	13.5
	60°	1076/30	24	24
	45°	--	--	--
	30°	1360/10	90	67
Ta	135°	698/100	5.6	5.6
	90°	647/40	13.0	13.0
	60°	750/30	20.0	20.0
	45°	1062/20	43	38
	30°	950/10	76	57
Sn	135°	2041/100	7.8	7.8
	90°	1427/40	14.0	14.0
	60°	1838/30	24	24
	45°	1965/20	38	35
	30°	1688/10	66	50

fifth column is derived from the fourth column by applying the correction for slit scattering and beam contamination described in section (6).

Figures 11, 12, 13, and 14 are plotted from the data contained in the fifth column of Table III. The errors indicated are of the type, described in the last section, which would not cancel out in a comparison of the differential or total cross sections of the various elements.

8. Total Cross Sections

Total cross sections are calculated according to the method described in section (5). In order to do this, estimates must be made, for the differential cross section for Au at 45° by interpolation, and for the 15° cross sections for all the elements by extrapolation. The estimates are shown in Table IV.

Table IV

Element	Angle	$\frac{d\sigma}{d\Omega}$ assumed
Au	45°	44 millibarns
Pb	15°	110 "
Au	15°	110 "
Ta	15°	90 "
Sn	15°	70 "

The results of the calculation of total cross sections are given in Table V.

Table V

Element	σ total
Pb	0.29 barns
Au	0.29 "
Ta	0.25 "
Sn	0.25 "

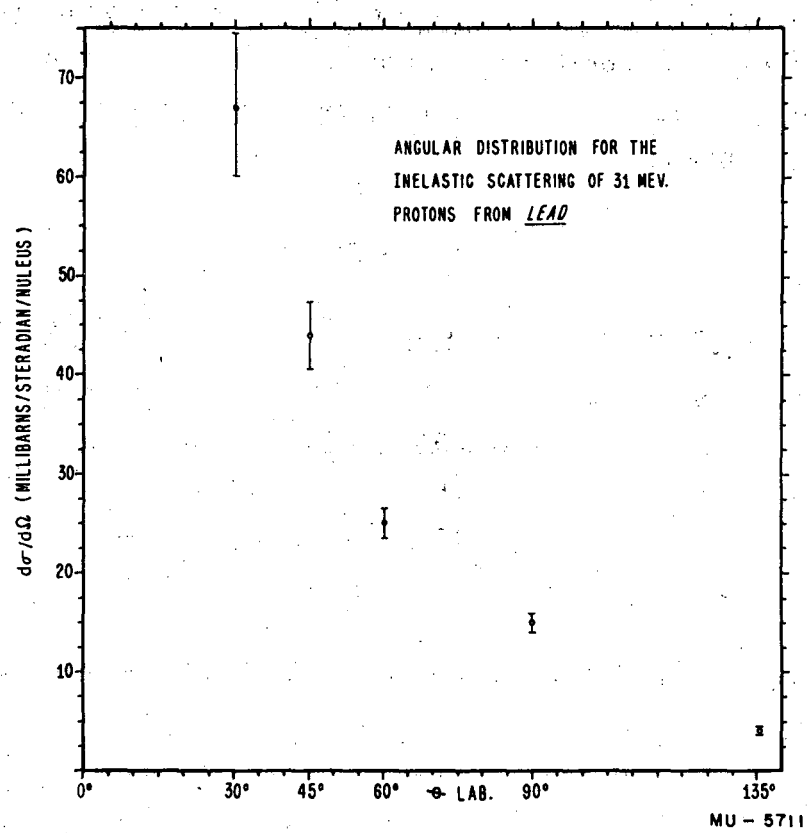
ANGULAR DISTRIBUTION FOR THE
INELASTIC SCATTERING OF 31 MEV.
PROTONS FROM LEAD
dσ/dΩ (MILLIBARNS/STERADIAN/NULEUS)
70
60
50
40
30
20
10
0°
30°
45°
60°
θ LAB.
90°
135°
MU - 5711

Fig. 11

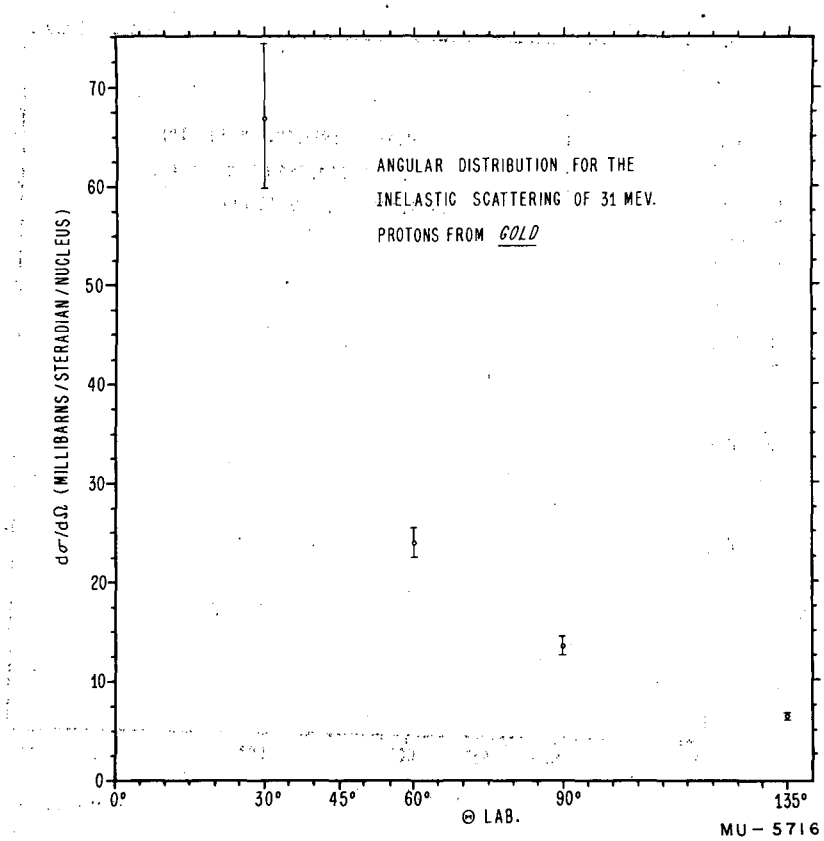
ANGULAR DISTRIBUTION FOR THE
INELASTIC SCATTERING OF 31 MEV.
PROTONS FROM GOLD
dσ/dΩ (MILLIBARNS/STERADIAN/NUCLEUS)
0
10
20
30
40
50
60
70
0°
30°
45°
60°
90°
135°
Θ LAB.
MU-5716

Fig. 12

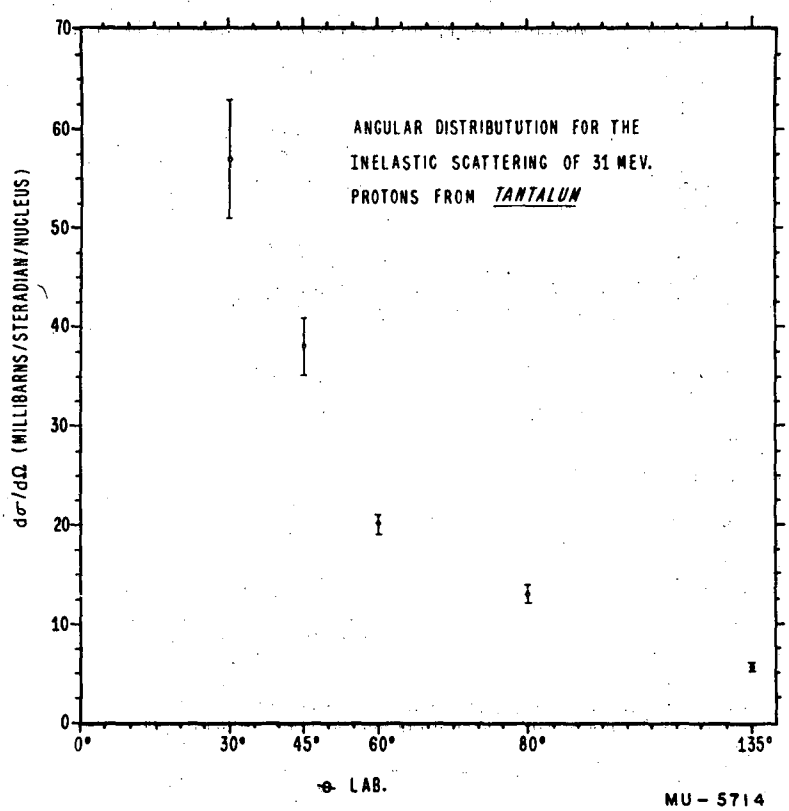
ANGULAR DISTRIBUTUTION FOR THE
INELASTIC SCATTERING OF 31 MEV.
PROTONS FROM TANTALUM
dσ/dΩ (MILLIBARNS/STERADIAN/NUCLEUS)
70
60
50
40
30
20
10
0
0°
30°
45°
60°
80°
135°
θ LAB.
MU-5714

Fig. 13

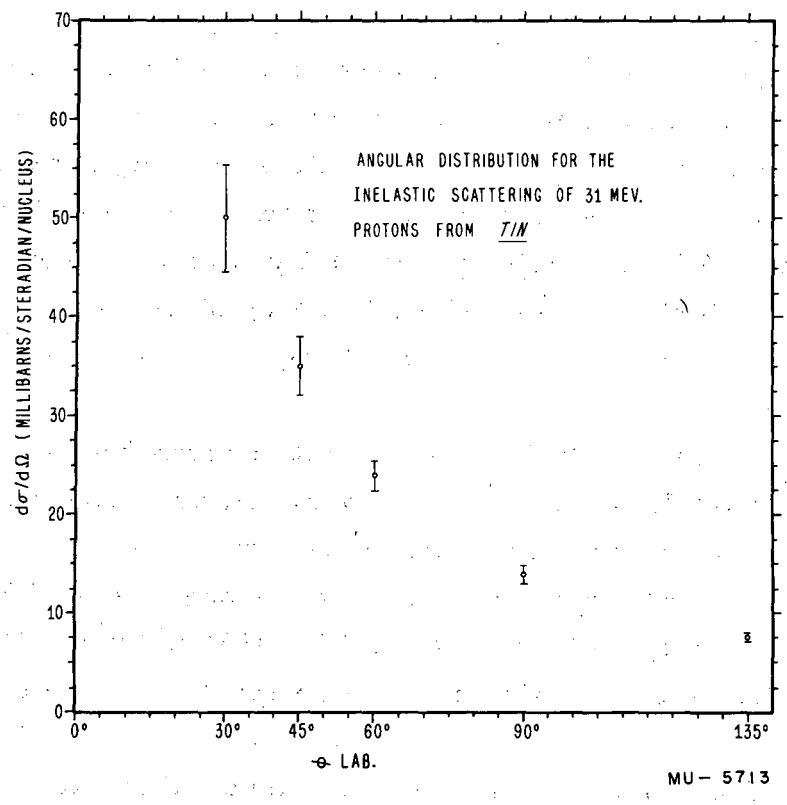
ANGULAR DISTRIBUTION FOR THE
INELASTIC SCATTERING OF 31 MEV.
PROTONS FROM TIN
dσ/dΩ (MILLIBARNS/STERADIAN/NUCLEUS)
0
10
20
30
40
50
60
70
0°
30°
45°
60°
90°
135°
θ LAB.
MU- 5713

Fig. 14

The probable error for the total cross sections, not including errors which would cancel out in taking the ratios of the total cross sections, is ± 10 percent.

The probable error for any of the total cross sections, including all known sources of error, is $^{+25\%}_{-20\%}$. In calculating this, it was assumed that the actual value of the 15° cross section lies between two times and one half times the assumed value.

IV. CONCLUSIONS

This experiment provides three pieces of information: (a) the energy distribution of protons inelastically scattered from heavy elements, (b) the angular distribution for the inelastic scattering of protons from heavy elements, and (c) the total cross section for these inelastic scattering processes. All three point to one easily recognized conclusion -- the inelastic scattering process which is taking place has nothing to do with the compound nucleus. The arguments involved in reaching this conclusion are:

(1) The relatively flat energy distributions are very different from the exponential distributions which would characterize the evaporation of nucleons from an excited compound nucleus.

(2) The angular distributions are strongly peaked forward (increasing by about a factor of ten in going from 135° to 30°). This is in contrast to the isotropic distribution one would expect from a compound nucleus process.

(3) The observed total cross sections, which are of the order of 15 percent of geometrical cross section, are at least an order of magnitude larger than the compound nucleus cross section for boiling off protons through the Coulomb barrier of a heavy nucleus.

This does not imply that this is a case in which the compound nucleus theory leads to incorrect results. Instead, what is apparently happening is that some additional process takes place which has a cross section so much larger than the compound nucleus cross section that the compound nucleus effects are completely hidden.

A model has been proposed which is capable of giving a qualitative explanation of the results of the experiment. According to the model, the inelastic scattering occurs when an incident proton collides with the rim of the nucleus.

Consider a 31 Mev proton incident upon a lead nucleus. The nucleus has a radius of $6\ r_o$, where $r_o = 1.4 \times 10^{-13}$ cm. The incident proton has a de Broglie wavelength, $\lambda\!\!\!^{-}$, of $\frac{2 r_o}{3}$. Consequently, it is legitimate to think of the proton as a small billiard ball colliding with a larger billiard ball, the nucleus. Now the mean free path of a proton (or neutron) in nuclear matter has been calculated from the known nucleon-nucleon cross section by Serber.[14] At 30 Mev, his calculation indicates that the mean free path approximately equals r_o. Thus, in any head-on collision with the nucleus, the incident proton will soon collide with the nucleons of the nucleus and rapidly share its kinetic energy with these nucleons. This event is just the one described by Bohr as being the first step in a compound nucleus process. However, in a collision in which the incident proton strikes the diffuse rim of the nucleus, it could collide with one or two nucleons, in such a manner that either the incident proton or one of the struck nucleons would escape carrying away a relatively large fraction of the kinetic energy. The diffuse region at the rim of a nucleus, in which the nucleon density decreases from its value inside a nucleus to the external value of zero, is said to have a thickness of the order of r_o.[15] This fuzzy region should behave, to some extent, like a collection of free nucleons because of the reduced average nucleon density in the region. Consequently, the collision of the incident proton may be considered approximately, as a collision between free nucleons.

The nucleon - nucleon collisions indicated by the model provide an explanation for the peaked forward character of the observed angular distributions. Consider a collision in which the incident proton strikes a nucleon at rest in the laboratory system. If the differential cross section for scattering is isotropic in the center of mass system of the two nucleons (a reasonable approximation for p - p or n - p scattering), then the differential cross section as seen in the laboratory system will be given by Fig. 15.

The differential cross section vanishes in the backward hemisphere because conservation of energy and momentum prohibit backward scatter-

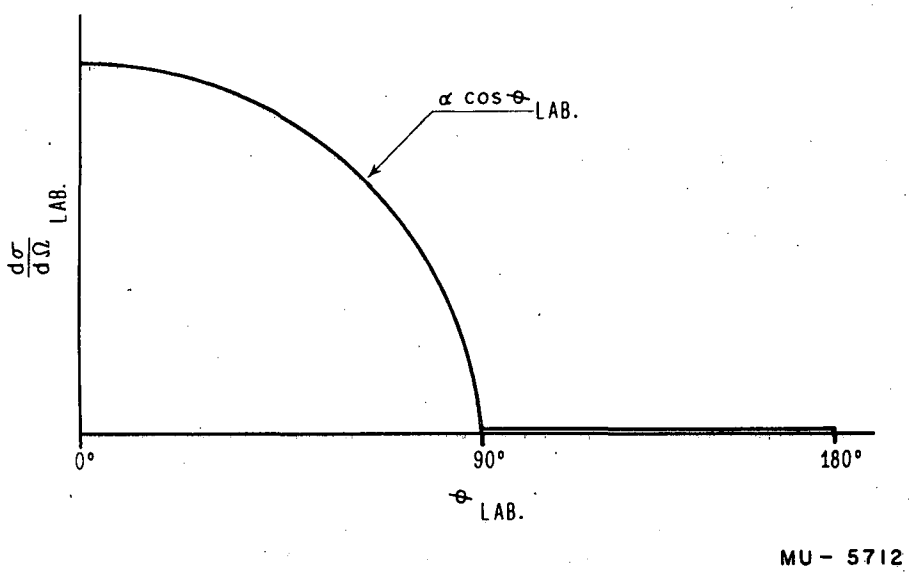

Fig. 15

ing in the laboratory system. If, next, one allows the struck nucleon to have an initial momentum distribution provided by its proximity to the rest of the nucleons in the nucleus, the differential cross section indicated above may well smooth out into something similar to the experimental results. For instance, the differential cross section would no longer vanish in the backward hemisphere since the incident proton may strike a nucleon with an initial backward component of momentum.

As the equation on page 7 indicates, the exponential character of the energy distribution of nucleons emitted from a compound nucleus is essentially due to the exponential form of the energy dependence of the density of states of a nucleon bound to a nucleus. A calculation of the expected energy distribution for the nucleon - nucleon collision process indicated by the model would result in an equation similar to that of page 7. However, in this case, the density of states to be used would probably be closely related to the density of states for a free particle. The density of states for a free particle (the familiar p^2dp factor) varies only slowly with energy. Consequently, the energy distribution would have only a relatively weak energy dependence (compared to an exponential dependence). This checks with the observed energy distribution.

Finally, the model can be used to predict the magnitude of the total cross section and the dependence of the total cross section on the atomic weight of the nucleus.

The projected area of the diffuse rim is equal to the area of a ring of width r_o and with a diameter about equal to the diameter of the nucleus. The geometrical cross section of lead is equal to πR^2, where $R = 6r_o$. The area of the ring would be about $r_o 2\pi 6r_o$. The ratio of the area of the ring to the geometrical area of the nucleus is one to three. The observed cross sections are approximately 15 percent of geometrical. Thus, the cross section for the process indicated by the model could well be large enough to account for the experimentally observed cross sections.

The projected area of the diffuse rim can be expressed by the equation: Area = $r_o 2\pi R$, where R, the radius of the ring, is approximately equal to the radius of the nucleus. Since nuclear radii are proportional to $A^{1/3}$, the total cross section for the process predicted

by the model might be expected to have an $A^{1/3}$ dependence. In going from Sn to Pb, $A^{1/3}$ increases by 20 percent. This certainly agrees with the experimental evidence that the Pb total cross section is 15 percent greater than the Sn cross section.

Further confirmation of this model might be obtained by investigating the energy distribution of neutrons emitted from heavy elements bombarded by 31 Mev protons, and by looking for angular correlations between nucleons emitted from heavy elements when bombarded by 31 Mev protons.

V. ACKNOWLEDGMENTS

The author is pleased to acknowledge his indebtedness to:

Professor L. W. Alvarez for his interest and advice in all phases of this experiment.

Professor A. C. Helmholz for his helpful advice in the initial stages of the experiment.

Dr. G. J. Igo for collaborating in the performance of this experiment.

Dr. Warren Heckrotte for instructive discussions of the interpretation of the results.

The entire linear accelerator crew, under the direction of Robert Watt and Wendel Olsen.

VI. BIBLIOGRAPHY

1. E.H. Rhoderick, Proc. Roy. Soc. 201, 348 (1950)
   This paper contains an extensive bibliography of the earlier work on inelastic proton scattering from the light elements.
2. C.J. Baker, J.N. Dodd, and D.H. Simmons, Phys. Rev. 85, 1050 (1952)
3. H.E. Gove, and J.A. Harvey, Phys. Rev. 82, 658 (1951)
4. H.W. Fulbright, and R.R. Bush, Phys. Rev. 74, 1323 (1948)
5. C. Levinthal, E.A. Martinelli, and A. Silverman, Phys. Rev. 78, 199 (1950)
6. N. Bohr, Nature 137, 344 (1936)
7. V. Weisskopf, Phys. Rev. 52, 295 (1937)
8. L. Wolfenstein, Phys. Rev. 82, 690 (1951)
9. R. Britten, Phys. Rev. 88, 283 (1952)
10. R.M. Eisberg, and G.J. Igo, Bulletin Am. Phys. Soc., Vol. 27, Number 6, page 15.
11. W. Franzen, R.W. Peelle, and R. Sherr, Phys. Rev. 79, 742 (1950)
12. B. Rossi, High Energy Particles, Prentice-Hall, Inc., New York, 1952, page 29
13. G.J. Igo, D.D. Clark, and R.M. Eisberg, Phys. Rev. 89, 879 (1953)
14. R. Serber, Phys. Rev. 72, 1114 (1947)
15. H.A. Bethe, and R.F. Bacher, Rev. Mod. Phys. 8, 164 (1936)